Synthesis and Characterization of Lithium Chloro Hydride

Randell L. Mills
Andreas Voigt
Bala Dhandapani
Jiliang He
Alejandra Echezuria

BlackLight Power, Inc.
493 Old Trenton Road
Cranbury, NJ 08512

A novel inorganic hydride compound lithium chloro hydride, *LiHCl*, which comprises a high binding energy hydride ion was synthesized by reaction of atomic hydrogen with potassium metal and lithium chloride. Lithium chloro hydride was identified by time of flight secondary ion mass spectroscopy, X-ray photoelectron spectroscopy, ^1H nuclear magnetic resonance spectroscopy, and powder X-ray diffraction. Hydride ions with increased binding energies may form many novel compounds with broad applications such as the oxidant of a high voltage battery.

1

I. INTRODUCTION

From a solution of a Schrödinger-type wave equation with a nonradiative boundary condition based on Maxwell's equations, Mills predicts that atomic hydrogen may undergo a catalytic reaction with certain atomized elements and ions which singly or multiply ionize at integer multiples of the potential energy of atomic hydrogen, $27.2\ eV$, $m \cdot 27.2\ eV$ wherein m is an integer [1-47]. The highly exothermic reaction involves a nonradiative energy transfer to form a hydrogen atom that is lower in energy than unreacted atomic hydrogen that corresponds to a fractional principal quantum number $(n = \frac{1}{p} = \frac{1}{integer}$ replaces the well known parameter $n = $ integer in the Rydberg equation for hydrogen excited states).

One such atomic catalytic system involves potassium atoms. The first, second, and third ionization energies of potassium are $4.34066\ eV$, $31.63\ eV$, and $45.806\ eV$, respectively. The triple ionization $(t = 3)$ reaction of K to K^{3+}, then, has a net enthalpy of reaction of $81.7766\ eV$, which is equivalent to $3 \cdot 27.2\ eV$. It has been reported [21] that intense extreme ultraviolet (EUV) emission was observed from incandescently heated atomic hydrogen and the atomized potassium catalyst that generated an anomalous plasma at low temperatures (e.g. $\approx 10^3\ K$) and an extraordinary low field strength of about 1-2 V/cm. No emission was observed with potassium or hydrogen alone or when sodium replaced potassium with hydrogen.

Emission was observed from K^{3+} that confirmed the resonant nonradiative energy transfer of $3 \cdot 27.2\ eV$ from atomic hydrogen to atomic potassium. The products of the catalysis reaction, lower-energy hydrogen atoms, have binding energies of $m \cdot 27.2\ eV$. Thus, they may further serve as catalysts, and further catalytic transitions may occur: $n = \frac{1}{2} \rightarrow \frac{1}{3}, \frac{1}{3} \rightarrow \frac{1}{4}, \frac{1}{4} \rightarrow \frac{1}{5}$, and so on. In addition, each lower-energy hydrogen atom is predicted to be highly reactive intermediate to form a novel hydride ion corresponding to the particular atomic energy level. The predicted hydride ion of hydrogen catalysis by atomic potassium is the hydride ion $H^-(1/4)$. This ion was reported to be been observed

spectroscopically at $110\,nm$ corresponding to its predicted binding energy of $11.2\,eV$ [21].

A number of independent experimental observations lead to the conclusion that atomic hydrogen can exist in fractional quantum states that are at lower energies than the traditional "ground" ($n = 1$) state. Prior related studies that support the possibility of a novel reaction of atomic hydrogen which produces a chemically generated or assisted plasma and produces novel hydride compounds include extreme ultraviolet (EUV) spectroscopy [1, 2, 4, 11-17, 19-21, 24, 28, 32-34, 36, 37], characteristic emission from catalysis and the hydride ion products [4, 6, 9, 10, 16, 21, 24], lower-energy hydrogen emission [12-15, 19, 20], plasma formation [1, 2, 4, 6, 9, 16, 21, 24, 28, 32, 33, 35-37], Balmer α line broadening [2, 4-6, 9, 11-15, 18, 28], elevated electron temperature [2, 5, 11-14], anomalous plasma afterglow duration [1, 35-36], power generation [5, 9, 13-15, 17, 18, 23, 25, 45-47], and analysis of chemical compounds [3, 4, 10, 23, 29, 39-43]. In prior reports [29, 39, 41], novel inorganic alkali and alkaline earth hydrides of the formula MHX and $MHMX$ wherein M is the metal, X, is a singly negatively charged anion, and H comprises a novel high binding energy hydride ion were synthesized in a high temperature gas cell by reaction of atomic hydrogen with a catalyst and MX or MX_2 corresponding to an alkali metal or alkaline earth metal, respectively. We report on the synthesis and characterization of $LiHCl$ which is a new compound of this series.

EXPERIMENTAL

Synthesis

Lithium chloro hydride, $LiHCl$, was prepared in a stainless steel gas cell shown in Figure 1 comprising a Ni screen hydrogen dissociator (Belleville Wire Cloth Co., Inc.), potassium metal catalyst (Aldrich Chemical Company), and $LiCl$ (Aldrich Chemical Company 99.9 %) as the reactant. A 304-stainless steel cell was in the form of a tube having an internal cavity of 359 millimeters in length and 73 millimeters in diameter. The top end of the cell was welded to a high vacuum 4 5/8 inch bored through conflat flange. The mating blank conflat flange contained a single coaxial hole in which was welded a 3/8 inch diameter stainless steel tube that was 100 cm in length and contained an inner

coaxial tube of 1/8 inch diameter. A silver plated copper gasket was placed between the two flanges. The two flanges were held together with 10 circumferential bolts. The bottom of the 3/8 inch tube was flush with the bottom surface of the top flange. The outer tube served as a vacuum line from the cell and the inner tube served as a hydrogen or helium supply line to the cell. The cell was surrounded by four heaters. Concentric to the heaters was high temperature insulation (AL 30 Zircar). Each of the four heaters were individually thermostatically controlled.

The cylindrical wall of the cell was lined with two layers of Ni screen totaling 150 grams. 3 grams of crystalline LiCl was poured into the cell. About 0.5 grams of potassium metal was added to the cell under an argon atmosphere. The cell was then continuously evacuated with a high vacuum turbo pump to reach 50 mTorr measured by a pressure gauge (Varian Convector, Pirrani type). The cell was heated by supplying power to the heaters. The heater power of the largest heater was measured using a wattmeter (Clarke -Hess model 259). The temperature of the cell was measured with a type K thermocouple (Omega). The cell temperature was then slowly increased over 2 hours to 300 °C using the heaters that were controlled by a type 97000 controller. The power to the largest heater and the cell temperature and pressure were continuously recorded by a DAS. The vacuum pump valve was closed. Hydrogen was slowly added to maintain a pressure within the range of 1000 Torr to 1500 Torr. The temperature of the cell was then slowly increased to 550 °C over 5 hours. The hydrogen valve was closed except to maintain the pressure at 1500 Torr. After 72 hours, the temperature of the cell was reduced to 400 °C at a rate of 15 °C/hr. The hydrogen supply was switched to helium which was flowed through the inner supply line to the cell while a vacuum was pulled on the outer vacuum line to remove volatilized potassium metal at 400 °C. The cell was then cooled and opened. About 3 grams of light green/brown crystals were observed to have formed in the bottom of the cell.

ToF-SIMS Characterization

The crystalline samples were grounded into powder in a drybox, and then sprinkled onto the surface of a double-sided adhesive tape and characterized using Physical Electronics TRIFT ToF-SIMS instrument. The

4

primary ion source was a pulsed $^{69}Ga^+$ liquid metal source operated at 15 keV. The secondary ions were exacted by a ± 3 keV (according to the mode) voltage. Three electrostatic analyzers (Triple-Focusing-Time-of-Flight) deflect them in order to compensate for the initial energy dispersion of ions of the same mass. The 400 pA dc current was pulsed at a 5 kHz repetition rate with a 7 ns pulse width. The analyzed area was $60\,\mu m$ x $60\,\mu m$ and the mass range was 0-1000 AMU. The total ion dose was 7×10^{11} $ions/cm^2$, ensuring static conditions. Charge compensation was performed with a pulsed electron gun operated at 20 eV electron energy. In order to remove surface contaminants and expose a fresh surface for analysis, the samples were sputter-cleaned for 30 s using a $80\,\mu m$ x $80\,\mu m$ raster, with 600 pA current, resulting in a total ion dose of 10^{15} $ions/cm^2$. Three different regions on each sample of $60\,\mu m$ x $60\,\mu m$ were analyzed. The positive and negative SIMS spectra were acquired. Representative post sputtering data is reported. The ToF-SIMS data were treated using 'cadence' software (Physical Electronics), which calculates the mass calibration from well-defined reference peaks.

XPS Characterization

A series of XPS analyses of low binding energy region (0 to 100 eV) were made on the crystalline samples using a Scienta 300 XPS Spectrometer. The fixed analyzer transmission mode and the sweep acquisition mode were used. The step energy in the survey scan was $0.5\,eV$, and the step energy in the high resolution scan was $0.15\,eV$. In the survey scan, the time per step was 0.4 seconds, and the number of sweeps was 4. In the high resolution scan, the time per step was 0.3 seconds, and the number of sweeps was 30. $C\,1s$ at $284.5\,eV$ was used as the internal standard.

The binding energies and features of core level electrons of control $LiCl$ and the crystals comprising the $LiHCl$ sample were analyzed by a Kratos XSAM-800 spectrometer using nonmonochromatic $Al\,K\alpha$ (1468.6 eV) radiation. Samples were crushed in a glove box under argon and mounted on an analysis stub with copper tape. A piece of gold foil was stuck into the sample for calibration. The samples were transferred from glove box to sample treatment chamber under an inert atmosphere. A survey spectrum was run from 1000 eV to 0 eV. For quantitative

analysis, high resolution spectra were run on core level electrons of interest, $Li\,1s$ and $Cl\,2p$ electrons. A high resolution spectrum of the low binding energy region was also run from 120 eV to 0 eV that corresponded to the survey spectrum. Fixed analyzer transmission (FAT) mode was used in all measurements. For the survey scan, a pass energy of 320 eV was employed. A pass energy of 40 eV was used for high resolution scans. In the cases where a charging effect was observed, the spectrum was corrected by using a calibration of $Au\,4f_{7/2}$ peak at 84.0 eV as a first standard and the $C\,1s$ peak at 284.5 eV as a second standard.

NMR Spectroscopy

Solid state ^1H MAS NMR was performed on the samples using a custom built spectrometer operating with a Nicolet 1280 computer. Final pulse generation was from a tuned Henry radio amplifier. The ^1H NMR frequency was 270.6196 MHz. A $5\,\mu sec$ pulse corresponding to a 41° pulse length and a 3 second recycle delay were used. The window was $\pm 20\,kHz$. The spin speed was 4.0 kHz. The number of scans was 600. The offset was 1541.6 Hz, and the magnetic flux was 6.357 T. The samples were handled under a nitrogen atmosphere. Chemical shifts were referenced to external tetramethylsilane (TMS). The reference comprised LiH (Aldrich Chemical Company 99%) and equivalent molar mixtures of LiH (Aldrich Chemical Company 99%) and $LiCl$ (Aldrich Chemical Company 99.99%) prepared in a glove box under argon.

Characterization by X-ray Diffraction (XRD)

The XRD patterns were obtained by IC Laboratories (Amawalk, NY) using a Phillips 547 Diffractometer tuned for $Cu\,K_\alpha$ (1.540590 Å) radiation generated at 45 kV and 35 mA. The sample was scanned from 8 to 68 2-theta with a step size of 0.02° and 1 second per step.

RESULTS

ToF-SIMS

The positive ToF-SIMS spectra obtained from $LiHCl$ and $LiCl$ control are shown in Figures 2 and 3, respectively. The positive ion spectrum of $LiHCl$ and that of the $LiCl$ were dominated by the Li^+ ion. Ga^+ $m/z = 69$, K_2^+ $m/z = 78$, K_2H^+ $m/z = 79$, K_2O^+ $m/z = 94$, K_2OH^+ $m/z = 95$,

6

$K(KCl)^+$ $m/z = 113$, KCO_3^+ $m/z = 122$, $KHCO_3^+$ $m/z = 123$ and $K_3CO_3^+$ $m/z = 177$ were also observed in the *LiHCl* sample. The presence of K in the *LiHCl* sample was due to the addition of K metal as a catalyst in the synthesis of *LiHCl*.

The negative ion ToF-SIMS of the *LiHCl* shown in Figure 4 was dominated by H^-, O^- and Cl^- peaks. Oxygen contamination was from some air exposure during sample preparation. The Cl^- count was lower than H^-; whereas, Cl^- dominated the negative ion ToF-SIMS of the *LiCl* control shown in Figure 5. H^- $m/z = 1$, and O^- $m/z = 16$, were also observed in *LiCl*.

XPS

A survey spectrum was obtained over the region $E_b = 0\,eV$ to $1200\,eV$. The primary element peaks allowed for the determination of all of the elements present in the *LiHCl* and the control *LiCl*. The survey spectrum also detected shifts in the binding energies of the elements which had implications to the identity of the compound containing the elements.

The major species present in control *LiCl* were lithium and chlorine. The XPS survey scan of the *LiHCl* sample obtained on the Scienta instrument is shown in Figure 6. Potassium and oxygen from air exposure of the potassium catalyst during sample preparation was present as well as lithium. Chlorine was observed in the low binding energy region.

The 0-120 eV binding energy region of high resolution XPS spectra of the *LiHCl* sample (solid), the control *LiCl* (dashed), and the 0-30 eV region of an additional control *KCl* obtained on the Scienta instrument are shown in Figure 7. Elements present in the survey scan which could be assigned to peaks in the low binding energy region of the *LiHCl* sample were the $K\,3p$ and $K\,3s$ peaks at 19 eV and 35 eV, respectively, the $O\,2s$ at 24 eV, $Li\,1s$ at 55 eV, and the $Cl\,3p$ peak at 6.5 eV. Accordingly, any other peaks in this region must be due to novel species. The XPS spectrum of the *LiHCl* sample differs from those of *LiCl* and *KCl* by having additional features at 11.2 eV and 14.7 eV. *LiOH* was present in *LiCl* and the *LiHCl* sample as shown by the presence of $O\,2s$ in Figure 7. Thus, the novel peaks can not be assigned to *LiOH*.

7

The 0-120 eV binding energy region of high resolution XPS spectra of the *LiHCl* sample (solid) and the control *LiCl* (dashed) obtained on the Scienta instrument is shown in Figure 8. Hydrogen is the only element which does not have primary element peaks; thus, it is the only candidate to produce the novel peaks. The XPS peaks centered at 11.2 eV and 14.7 eV that do not correspond to any other primary element peaks may correspond to the $H^-(n = 1/4) E_b = 11.2 \, eV$ hydride ion predicted by Mills [38] (Eqs. (7-8)) in two different chemical environments where E_b is the predicted vacuum binding energy. In this case, the reaction to form $H^-(n = 1/4)$ is given by Eqs. (3-5) and Eq. (6). Figure 8 also shows that the *Li* ls peak of *LiHCl* was shifted about 1.7 eV to lower binding energies relative to the *Li* ls peak of *LiCl* possibly due to the presence of $H^-(n = 1/4)$.

The binding energies and features of core level electrons of control *LiCl* and the *LiHCl* sample were analyzed by XPS. The local structure of *LiCl* and the *LiHCl* sample was investigated by studying the metal *Li* ls core level electrons and the chloride *Cl* 2p core level electrons. As atomic hydrogen undergoes reaction with potassium catalyst to form a lower-energy hydrogen species which subsequently reacts with the lithium center in *LiCl*, alterations in the electronic structure of lithium such as changes in core level binding energies relative to the starting compound, *LiCl*, were expected.

The XPS spectra of the *Li* ls core level in *LiCl* and *LiHCl* appear in Figures 9A and 9B respectively. The *Li* ls binding energy (54.96 eV) in the *LiHCl* sample is about 1.7 eV lower than that of *Li* ls (56.66 eV) in the control *LiCl*. The full width at half maximum (FWHM) in *Li* ls from the *LiHCl* sample is about 0.17 eV broader than that from control *LiCl*. The presence of the novel hydride ion shifted the *Li* ls peaks to lower binding energies relative to the corresponding peaks of *LiCl*. A similar shift in the *Li* ls core level of the *LiHCl* sample was observed when compared to *Li* ls of *LiCl* recorded with the Scienta instrument as shown in Figure 8.

The XPS spectra of the *Cl* 2p core level in *LiCl* and *LiHCl* appear in Figures 10A and 10B respectively. In contrast to the *Li* ls core level, the *Cl* 2p core level FWHM in the *LiHCl* sample is very similar to *LiCl*. Comparing the alterations in the *Li* core level versus the *Cl* core level indicates that the lower-energy hydrogen species is bound to the metal

center of *LiCl*. This binding largely influences the metal core level with little perturbation of the halogen core level.

The XPS data clearly indicates a change in the electronic structure at the *Li* core level and different bonding in *LiHCl* relative to that in the corresponding *LiCl*. It strongly suggests the formation of a novel metal hydride which is consistent with the supporting data provided by XPS given above, NMR and ToF-SIMS given in the respective sections.

The XPS survey scans of *LiCl* and the *LiHCl* sample obtained on the Kratos instrument are shown in Figures 11A-B, respectively. The 0-100 eV binding energy region of high resolution XPS spectra of *LiCl* and the *LiHCl* sample obtained on the Kratos instrument are shown in Figures 12A-B, respectively. Hydrogen is the only element which does not have primary element peaks; thus, it is the only candidate to produce the shifted *Li* 1s peak of the *LiHCl* sample compared to *LiCl* as shown in Figures 12A-B.

NMR

The ^1H MAS NMR spectra of the *LiHCl* sample, the control comprising an equal molar mixture of *LiH* and *LiCl*, and the control *LiH* relative to external tetramethylsilane (TMS) are shown in Figures 13A-C, respectively. Ordinary hydride ion has resonances at 4.2 ppm and 1.1 ppm in the *LiH/ LiCl* mixture and in *LiH* alone as shown in Figures 13B and 13C, respectively. The presence of *LiCl* does not shift the resonance of ordinary hydride as shown in Figure 13B. The resonance at 4.2 ppm and 1.2 ppm which are assigned to ordinary hydride ion was observed in the spectrum of the *LiHCl* sample as shown in Figure 13A. A large distinct upfield resonance was observed at -15.2 ppm, and features were observed at -1.7 ppm and -9 ppm. These features were not observed in either control. The upfield shifted peaks are consistent with a hydride ion with a smaller radius as compared with ordinary hydride since a smaller radius increases the shielding or diamagnetism. This upfield shifted peak was assigned to a novel hydride ion of *LiHCl* in different chemical environments. The down field shifted peak at 13.3 ppm may have been due to H^+ stabilized by the novel H^-.

XRD

The XRD pattern of *LiHCl* is shown in Figure 14. The identifiable peaks corresponded to a mixture of *LiH*, *LiO* and *LiOH*. In addition, the spectrum contained a number of peaks that could not be assigned. The 2-theta and d-spacings of the unidentified XRD peaks of the *LiHCl* sample are given in Table 1.

DISCUSSION

The ToF-SIMS of the product of the reaction of atomic hydrogen with potassium metal and *LiCl* showed Li^+ and H^- as the dominant peaks with Cl^- present. The potassium metal was oxidized by air exposure during sample preparation. The ToF-SIMS results recorded on the reaction product are consistent with the proposed structure *LiHCl*. The NMR and XPS data indicate that a novel hydride ion was present. The known compounds *LiCl* and *LiH* have the lithium ion in a +1 state. The compound *LiHCl* is unknown and extraordinary. The implied valence of lithium is +2.

The 0-100 eV binding energy region of a high resolution XPS spectrum of the *LiHCl* sample indicates the presence of the hydride ion $H^-(1/4)$ with binding energies of 11.2 eV and 14.7 eV compared to the predicted binding energy of 11.2 eV. The presence of two peaks may have been due to the presence $H^-(1/4)$ in two different chemical environments. The XPS data of the core levels clearly indicates a change in the electronic structure and different bonding in *LiHCl* relative to that in the corresponding *LiCl*. This binding influences the metal core level with little perturbation of the halogen core level. Comparing the alterations in the *Li* core levels versus the *Cl* core level indicates that the lower-energy hydrogen species binds to the metal center of *LiCl*. The presence of the novel hydride ion shifts the *Li* 1s peaks to lower binding energies relative to the corresponding peaks of *LiCl*. It strongly suggests the formation of a novel metal hydride which is consistent with the supporting data provided by XPS , NMR and ToF-SIMS.

The resonances in the NMR spectrum of the *LiHCl* at 4.2 ppm and 1.1 ppm were assigned to ordinary hydride ion. The large distinct upfield resonance at -15.2 ppm, and features observed at -1.7 ppm and

1 0

-9 ppm identifies a hydride ion with a substantially smaller radius as compared with ordinary hydride since a smaller radius increases the shielding or diamagnetism, and the shift was extraordinary. *LiHCl* was possibly present in different chemical environments as evidenced by the three distinct upfield shifts.

XRD peaks were observed which did not match those known which supported the identification of a novel compound.

CONCLUSIONS

The ToF-SIMS, XPS and NMR results confirmed the identification of *LiHCl* with a hydride ion $H^-(1/4)$ having a high binding energy of 11.2 eV (Eqs. (7-8)) that matched theoretical predictions [38]. Hydride ion ($H^-(1/4)$) may be formed according to Eqs. (3-5) and Eq. (6) which was supported by the XPS and NMR data of the *LiHCl* sample. The identification of compounds containing novel hydride ions is indicative of a new field of hydrogen chemistry. Novel hydride ions may combine with other cations such as other alkali cations and alkaline earth, rare earth, and transition element cations. Numerous novel compounds may be synthesized with extraordinary properties relative to the corresponding compounds having ordinary hydride ions [3, 4, 10, 23, 29, 39-43]. These novel compounds may have a breath of applications. For example, a high voltage battery according to the hydride binding energies in *LiHCl* and previously observed by XPS [3, 10, 23, 39-43] may be possible having projected specifications that are significantly exceed those of the current state of the art [7, 40, 42].

APPENDIX

Mills [38] predicted an exothermic reaction whereby certain atoms or ions serve as catalysts to release energy from hydrogen to produce an increased binding energy hydrogen atom called a hydrino having a binding energy of

$$Binding\ Energy = \frac{13.6\ eV}{\left(\frac{1}{p}\right)^2} \qquad (1)$$

where p is an integer greater than 1, designated as $H\left[\dfrac{a_H}{p}\right]$ where a_H is the radius of the hydrogen atom. Hydrinos were predicted to form by reacting an ordinary hydrogen atom with a catalyst having a net enthalpy of reaction of about

$$m \cdot 27.2\ eV \qquad (2)$$

where m is an integer. This catalysis releases energy from the hydrogen atom with a commensurate decrease in size of the hydrogen atom, $r_n = na_H$. For example, the catalysis of $H(n=1)$ to $H(n=1/2)$ releases $40.8\ eV$, and the hydrogen radius decreases from a_H to $\frac{1}{2}a_H$.

A catalytic system is provided by the ionization of t electrons from an atom each to a continuum energy level such that the sum of the ionization energies of the t electrons is approximately $m\,X\,27.2\ eV$ where m is an integer. One such catalytic system involves potassium. The first, second, and third ionization energies of potassium are $4.34066\ eV$, $31.63\ eV$, $45.806\ eV$, respectively [48]. The triple ionization ($t=3$) reaction of K to K^{3+}, then, has a net enthalpy of reaction of $81.7426\ eV$, which is equivalent to $m=3$ in Eq. (2).

$$81.7426\ eV + K(m) + H\left[\frac{a_H}{p}\right] \rightarrow K^{3+} + 3e^- + H\left[\frac{a_H}{(p+3)}\right] + [(p+3)^2 - p^2]X13.6\ eV \qquad (3)$$

$$K^{3+} + 3e^- \rightarrow K(m) + 81.7426\ eV \qquad (4)$$
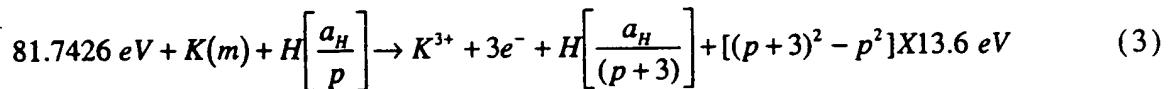
And, the overall reaction is

$$H\left[\frac{a_H}{p}\right] \rightarrow H\left[\frac{a_H}{(p+3)}\right] + [(p+3)^2 - p^2]X13.6\ eV \qquad (5)$$

12
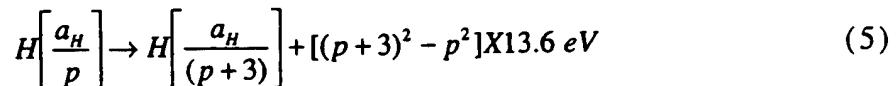
A novel hydride ion having extraordinary chemical properties given by Mills [38] was predicted to form by the reaction of an electron with a hydrino (Eq. (6)). The resulting hydride ion is referred to as a hydrino hydride ion, designated as $H^-(1/p)$.

$$H\left[\frac{a_H}{p}\right] + e^- \rightarrow H^-(1/p) \qquad (6)$$

The hydrino hydride ion is distinguished from an ordinary hydride ion having a binding energy of 0.8 eV. The latter is hereafter referred to as "ordinary hydride ion". The hydrino hydride ion is predicted [38] to comprise a hydrogen nucleus and two indistinguishable electrons at a binding energy according to the following formula:

$$Binding\ Energy = \frac{\hbar^2 \sqrt{s(s+1)}}{8\mu_e a_0^2 \left[\frac{1+\sqrt{s(s+1)}}{p}\right]^2} - \frac{\pi\mu_0 e^2 \hbar^2}{m_e^2 a_0^3}\left(1 + \frac{2^2}{\left[\frac{1+\sqrt{s(s+1)}}{p}\right]^3}\right) \qquad (7)$$

where p is an integer greater than one, $s = 1/2$, $\hbar$ is Planck's constant bar, μ_o is the permeability of vacuum, m_e is the mass of the electron, μ_e is the reduced electron mass, a_o is the Bohr radius, and e is the elementary charge. The ionic radius is

$$r_1 = \frac{a_0}{p}\left(1 + \sqrt{s(s+1)}\right); \ s = \frac{1}{2} \qquad (8)$$

From Eq. (8), the radius of the hydrino hydride ion $H^-(1/p); p = $ integer is $\frac{1}{p}$ that of ordinary hydride ion, $H^-(1/1)$.

13

REFERENCES

1. H. Conrads, R. Mills, Th. Wrubel, "Emission in the Deep Vacuum Ultraviolet from an Incandescently Driven Plasma in a Potassium Carbonate Cell", Plasma Sources Science and Technology, submitted.

2. R. L. Mills, P. Ray, "Stationary Inverted Lyman Population Formed from Incandescently Heated Hydrogen Gas with Certain Catalysts", Chem. Phys. Letts., submitted.

3. R. L. Mills, B. Dhandapani, J. He, "Synthesis and Characterization of a Highly Stable Amorphous Silicon Hydride", Int. J. Hydrogen Energy, submitted.

4. R. L. Mills, P. Ray, R. Mayo, "CW HI Laser Based on a Stationary Inverted Lyman Population Formed from Incandescently Heated Hydrogen Gas with Certain Catalysts", IEEE Transactions on Plasma Science, submitted.

5. R. L. Mills, P. Ray, "Substantial Changes in the Characteristics of a Microwave Plasma Due to Combining Argon and Hydrogen", New Journal of Physics, submitted.

6. R. L. Mills, P. Ray, " High Resolution Spectroscopic Observation of the Bound-Free Hyperfine Levels of a Novel Hydride Ion Corresponding to a Fractional Rydberg State of Atomic Hydrogen", Int. J. Hydrogen Energy, in press.

7. R. L. Mills, E. Dayalan, "Novel Alkali and Alkaline Earth Hydrides for High Voltage and High Energy Density Batteries", Proceedings of the 17th Annual Battery Conference on Applications and Advances, California State University, Long Beach, CA, (January 15-18, 2002), in press.

8. R. Mayo, R. Mills, M. Nansteel, "On the Potential of Direct and MHD Conversion of Power from a Novel Plasma Source to Electricity for Microdistributed Power Applications", IEEE Transactions on Plasma Science, submitted.

9. R. Mills, P. Ray, J. Dong, M. Nansteel, W. Good, P. Jansson, B. Dhandapani, J. He, "Excessive Balmer α Line Broadening, Power Balance, and Novel Hydride Ion Product of Plasma Formed from Incandescently Heated Hydrogen Gas with Certain Catalysts", Int. J. Hydrogen Energy, submitted.

10. R. Mills, E. Dayalan, P. Ray, B. Dhandapani, J. He, "Highly Stable Novel Inorganic Hydrides from Aqueous Electrolysis and Plasma Electrolysis, Japanese Journal of Applied Physics, submitted.

11. R. L. Mills, P. Ray, B. Dhandapani, J. He, "Comparison of Excessive Balmer α Line Broadening of Glow Discharge and Microwave Hydrogen Plasmas with Certain Catalysts", Chem. Phys., submitted.

12. R. L. Mills, P. Ray, B. Dhandapani, J. He, "Spectroscopic Identification of Fractional Rydberg States of Atomic Hydrogen", J. of Phys. Chem., submitted.

13. R. L. Mills, P. Ray, B. Dhandapani, M. Nansteel, X. Chen, J. He, "New Power Source from Fractional Rydberg States of Atomic Hydrogen", Chem. Phys. Letts., submitted.

14. R. L. Mills, P. Ray, B. Dhandapani, M. Nansteel, X. Chen, J. He, "Spectroscopic Identification of Transitions of Fractional Rydberg States of Atomic Hydrogen", Quantitative Spectroscopy and Energy Transfer, submitted.

15. R. L. Mills, P. Ray, B. Dhandapani, M. Nansteel, X. Chen, J. He, "New Power Source from Fractional Quantum Energy Levels of Atomic Hydrogen that Surpasses Internal Combustion", Spectrochimica Acta, Part A, submitted.

16. R. L. Mills, P. Ray, "Spectroscopic Identification of a Novel Catalytic Reaction of Rubidium Ion with Atomic Hydrogen and the Hydride Ion Product", Int. J. Hydrogen Energy, in press.

17. R. Mills, J. Dong, W. Good, P. Ray, J. He, B. Dhandapani, Measurement of Energy Balances of Noble Gas-Hydrogen Discharge Plasmas Using Calvet Calorimetry, Int. J. Hydrogen Energy, in press.

18. R. L. Mills, A. Voigt, P. Ray, M. Nansteel, B. Dhandapani, "Measurement of Hydrogen Balmer Line Broadening and Thermal Power Balances of Noble Gas-Hydrogen Discharge Plasmas", Int. J. Hydrogen Energy, in press.

19. R. Mills, P. Ray, "Vibrational Spectral Emission of Fractional-Principal-Quantum-Energy-Level Hydrogen Molecular Ion", Int. J. Hydrogen Energy, in press.

20. R. Mills, P. Ray, "Spectral Emission of Fractional Quantum Energy Levels of Atomic Hydrogen from a Helium-Hydrogen Plasma and the

Implications for Dark Matter", Int. J. Hydrogen Energy, Vol. 27, No. 3, pp. 301-322.

21. R. Mills, P. Ray, "Spectroscopic Identification of a Novel Catalytic Reaction of Potassium and Atomic Hydrogen and the Hydride Ion Product", Int. J. Hydrogen Energy, Vol. 27, No. 2, February, (2002), pp. 183-192.

22. R. Mills, "BlackLight Power Technology-A New Clean Hydrogen Energy Source with the Potential for Direct Conversion to Electricity", Proceedings of the National Hydrogen Association, 12 th Annual U.S. Hydrogen Meeting and Exposition, *Hydrogen: The Common Thread*, The Washington Hilton and Towers, Washington DC, (March 6-8, 2001), pp. 671-697.

23. R. Mills, W. Good, A. Voigt, Jinquan Dong, "Minimum Heat of Formation of Potassium Iodo Hydride", Int. J. Hydrogen Energy, Vol. 26, No. 11, Oct., (2001), pp. 1199-1208.

24. R. Mills, "Spectroscopic Identification of a Novel Catalytic Reaction of Atomic Hydrogen and the Hydride Ion Product", Int. J. Hydrogen Energy, Vol. 26, No. 10, (2001), pp. 1041-1058.

25. R. Mills, N. Greenig, S. Hicks, "Optically Measured Power Balances of Anomalous Discharges of Mixtures of Argon, Hydrogen, and Potassium, Rubidium, Cesium, or Strontium Vapor", Int. J. Hydrogen Energy, in press.

26. R. Mills, "The Grand Unified Theory of Classical Quantum Mechanics", Global Foundation, Inc. Orbis Scientiae entitled *The Role of Attractive and Repulsive Gravitational Forces in Cosmic Acceleration of Particles The Origin of the Cosmic Gamma Ray Bursts*, (29th Conference on High Energy Physics and Cosmology Since 1964) Dr. Behram N. Kursunoglu, Chairman, December 14-17, 2000, Lago Mar Resort, Fort Lauderdale, FL, Kluwer Academic/Plenum Publishers, New York, pp. 243-258.

27. R. Mills, "The Grand Unified Theory of Classical Quantum Mechanics", Int. J. Hydrogen Energy, in press.

28. R. Mills and M. Nansteel, P. Ray, "Argon-Hydrogen-Strontium Discharge Light Source", IEEE Transactions on Plasma Science, in press.

29. R. Mills, B. Dhandapani, M. Nansteel, J. He, A. "Voigt, Identification of Compounds Containing Novel Hydride Ions by Nuclear Magnetic

Resonance Spectroscopy", Int. J. Hydrogen Energy, Vol. 26, No. 9, Sept. (2001), pp. 965-979.

30. R. Mills, "BlackLight Power Technology-A New Clean Energy Source with the Potential for Direct Conversion to Electricity", Global Foundation International Conference on "Global Warming and Energy Policy", Dr. Behram N. Kursunoglu, Chairman, Fort Lauderdale, FL, November 26-28, 2000, Kluwer Academic/Plenum Publishers, New York, pp. 1059-1096.

31. R. Mills, The Nature of Free Electrons in Superfluid Helium--a Test of Quantum Mechanics and a Basis to Review its Foundations and Make a Comparison to Classical Theory, Int. J. Hydrogen Energy, Vol. 26, No. 10, (2001), pp. 1059-1096.

32. R. Mills, M. Nansteel, and Y. Lu, "Excessively Bright Hydrogen-Strontium Plasma Light Source Due to Energy Resonance of Strontium with Hydrogen", Plasma Chemistry and Plasma Processing, submitted.

33. R. Mills, J. Dong, Y. Lu, "Observation of Extreme Ultraviolet Hydrogen Emission from Incandescently Heated Hydrogen Gas with Certain Catalysts", Int. J. Hydrogen Energy, Vol. 25, (2000), pp. 919-943.

34. R. Mills, "Observation of Extreme Ultraviolet Emission from Hydrogen-KI Plasmas Produced by a Hollow Cathode Discharge", Int. J. Hydrogen Energy, Vol. 26, No. 6, (2001), pp. 579-592.

35. R. Mills, "Temporal Behavior of Light-Emission in the Visible Spectral Range from a Ti-K2CO3-H-Cell", Int. J. Hydrogen Energy, Vol. 26, No. 4, (2001), pp. 327-332.

36. R. Mills, T. Onuma, and Y. Lu, "Formation of a Hydrogen Plasma from an Incandescently Heated Hydrogen-Catalyst Gas Mixture with an Anomalous Afterglow Duration", Int. J. Hydrogen Energy, Vol. 26, No. 7, July, (2001), pp. 749-762.

37. R. Mills, M. Nansteel, and Y. Lu, "Observation of Extreme Ultraviolet Hydrogen Emission from Incandescently Heated Hydrogen Gas with Strontium that Produced an Anomalous Optically Measured Power Balance", Int. J. Hydrogen Energy, Vol. 26, No. 4, (2001), pp. 309-326.

38. R. Mills, The Grand Unified Theory of Classical Quantum Mechanics, September 2001 Edition, BlackLight Power, Inc., Cranbury, New Jersey, Distributed by Amazon.com.

17

39. R. Mills, B. Dhandapani, N. Greenig, J. He, "Synthesis and Characterization of Potassium Iodo Hydride", Int. J. of Hydrogen Energy, Vol. 25, Issue 12, December, (2000), pp. 1185-1203.

40. R. Mills, "Novel Inorganic Hydride", Int. J. of Hydrogen Energy, Vol. 25, (2000), pp. 669-683.

41. R. Mills, B. Dhandapani, M. Nansteel, J. He, T. Shannon, A. Echezuria, "Synthesis and Characterization of Novel Hydride Compounds", Int. J. of Hydrogen Energy, Vol. 26, No. 4, (2001), pp. 339-367.

42. R. Mills, "Highly Stable Novel Inorganic Hydrides", Journal of New Materials for Electrochemical Systems, in press.

43. R. Mills, "Novel Hydrogen Compounds from a Potassium Carbonate Electrolytic Cell", Fusion Technology, Vol. 37, No. 2, March, (2000), pp. 157-182.

44. R. Mills, "The Hydrogen Atom Revisited", Int. J. of Hydrogen Energy, Vol. 25, Issue 12, December, (2000), pp. 1171-1183.

45. R. Mills, W. Good, "Fractional Quantum Energy Levels of Hydrogen", Fusion Technology, Vol. 28, No. 4, November, (1995), pp. 1697-1719.

46. R. Mills, W. Good, R. Shaubach, "Dihydrino Molecule Identification", Fusion Technology, Vol. 25, 103 (1994).

47. R. Mills and S. Kneizys, Fusion Technol. Vol. 20, 65 (1991).

48. David R. Linde, CRC Handbook of Chemistry and Physics, 79 th Edition, CRC Press, Boca Raton, Florida, (1998-9), p. 10-175 to p. 10-177.

Table 1. The 2-theta and d-spacings of the unidentified XRD peaks of the *LiHCl* sample.

Peak Number	2 – Theta (Deg)	d (Å)
2	26.60	3.3518
3	26.96	3.3066
4	30.70	2.9128
11	45.71	1.9849
12	49.26	1.8497
16	62.21	1.4923

Figure 1. Stainless steel gas cell.

Figure 2. The positive ToF-SIMS spectrum ($m/e = 0 - 200$) of the *LiHCl* sample that shows Li^+ as the dominate positive ion.

Figure 3. The positive ToF-SIMS spectrum ($m/e = 0 - 200$) of *LiCl* that shows Li^+ as the dominate positive ion.

Figure 4. The negative ToF-SIMS spectrum ($m/e = 0 - 200$) of the *LiHCl* sample that shows H^- as the dominate negative ion.

Figure 5. The negative ToF-SIMS spectrum ($m/e = 0 - 200$) of *LiCl* that shows Cl^- as the dominate negative ion.

Figure 6. The XPS survey scan of the *LiHCl* sample obtained on the Scienta instrument that shows the presence of potassium and oxygen from air exposure of the potassium catalyst during sample preparation as well as lithium.

Figure 7. The 0-120 eV binding energy region of high resolution XPS spectra of the *LiHCl* sample (solid), the control *LiCl* (dashed), and the 0-30 eV region of an additional control *KCl* obtained on the Scienta instrument. The XPS peaks centered at 11.2 eV and 14.7 eV can not be assigned to *LiCl*, *KCl*, or *LiOH*.

Figure 8. The 0-120 eV binding energy region of high resolution XPS spectra of the *LiHCl* sample (solid) and the control *LiCl* (dashed) obtained on the Scienta instrument. The XPS peaks centered at 11.2 eV and 14.7 eV that do not correspond to any other primary element peaks may correspond to the $H^-(n = 1/4) E_b = 11.2 \, eV$ possibly in two different chemical environments where E_b is the predicted vacuum binding energy. The *Li* 1s peak of *LiHCl* is shifted about 1.7 eV to lower binding energies relative to the *Li* 1s peak of *LiCl* possibly due to the presence of $H^-(n = 1/4)$.

Figure 9A. The XPS spectrum of the *Li* 1s core level in *LiCl* obtained on the Kratos instrument.

Figure 9B. The XPS spectrum of the *Li* 1s core level in *LiHCl* obtained on the Kratos instrument. The *Li* 1s binding energy (54.96 eV) in the *LiHCl* sample is about 1.7 eV lower than that of *Li* 1s (56.66 eV) in the control *LiCl*. The full width at half maximum (FWHM) in *Li* 1s from the *LiHCl* sample is about 0.17 eV broader than that from control *LiCl*.

Figure 10A. The XPS spectrum of the *Cl 2p* core level in *LiCl* obtained on the Kratos instrument.

Figure 10B. The XPS spectrum of the *Cl 2p* core level in *LiHCl* obtained on the Kratos instrument.

Figure 11A. The XPS survey scan of *LiCl* obtained on the Kratos instrument.

Figure 11B. The XPS survey scan of the *LiHCl* sample obtained on the Kratos instrument. The *Cl* 2p core level FWHM in the *LiHCl* sample is very similar to that of *LiCl*.

Figure 12A. The 0-100 eV binding energy region of a high resolution XPS spectrum of *LiCl* obtained on the Kratos instrument.

Figure 12B. The 0-100 eV binding energy region of a high resolution XPS spectrum of the *LiHCl* sample obtained on the Kratos instrument. Hydrogen is the only element which does not have primary element peaks; thus, it is the only candidate to produce the shifted *Li* 1s peak.

Figure 13A. The ^1H MAS NMR spectrum of *LiHCl* relative to external tetramethylsilane (TMS). The resonances at 4.2 ppm and 1.1 ppm were assigned to ordinary hydride ion. The large distinct upfield resonance at -15.2 ppm, and features observed at -1.7 ppm and -9 ppm identified a hydride ion with a substantially smaller radius as compared with ordinary hydride since a smaller radius increases the shielding or diamagnetism. The upfield peaks were assigned to a novel hydride ion of *LiHCl* possibly in different chemical environments.

Figure 13B. The ^1H MAS NMR spectrum of the control comprising an equal molar mixture of *LiH* and *LiCl* relative to external tetramethylsilane (TMS). Ordinary hydride ion has resonances at 4.2 ppm and 1.1 ppm in the *LiH/ LiCl* mixture and in *LiH*. The presence of *LiCl* does not shift the resonance of ordinary hydride as shown in Figure 13C.

Figure 13C. The ^1H MAS NMR spectrum of the control *LiH* relative to external tetramethylsilane (TMS).

Figure 14. The X-ray Diffraction (XRD) pattern of the *LiHCl* sample. Unidentified XRD peaks of *LiHCl* are given in Table 1.

H$_2$/He

Reactants

Stainless Steel
Reactor

H$_2$ Dissociator

Heater

Vacuum

Fig. 1

Fig. 2

LICL002.TDC + Ions 61μm 771495 cts LiCl,

Fig. 3

Fig. 4

Fig. 5

Fig. 6

Fig. 7

Fig. 8

Fig. 9

Fig. 10

Panel A:

Name	Pos.	FWHM	L.Sh.	Area	%
Cl 2p	198.949	2.30634	GL(30)	24332.2	63.36
Cl 2p	200.602	2.28726	GL(30)	14073.7	36.64

Cl 2p

CPS ×10³

Binding Energy (eV)

Panel B:

Name	Pos.	FWHM	L.Sh.	Area	%
Cl 2p	198.9	1.97317	GL(30)	169.0	60.44
Cl 2p	200.611	1.95004	GL(30)	110.6	39.56

Cl 2p

CPS ×10¹
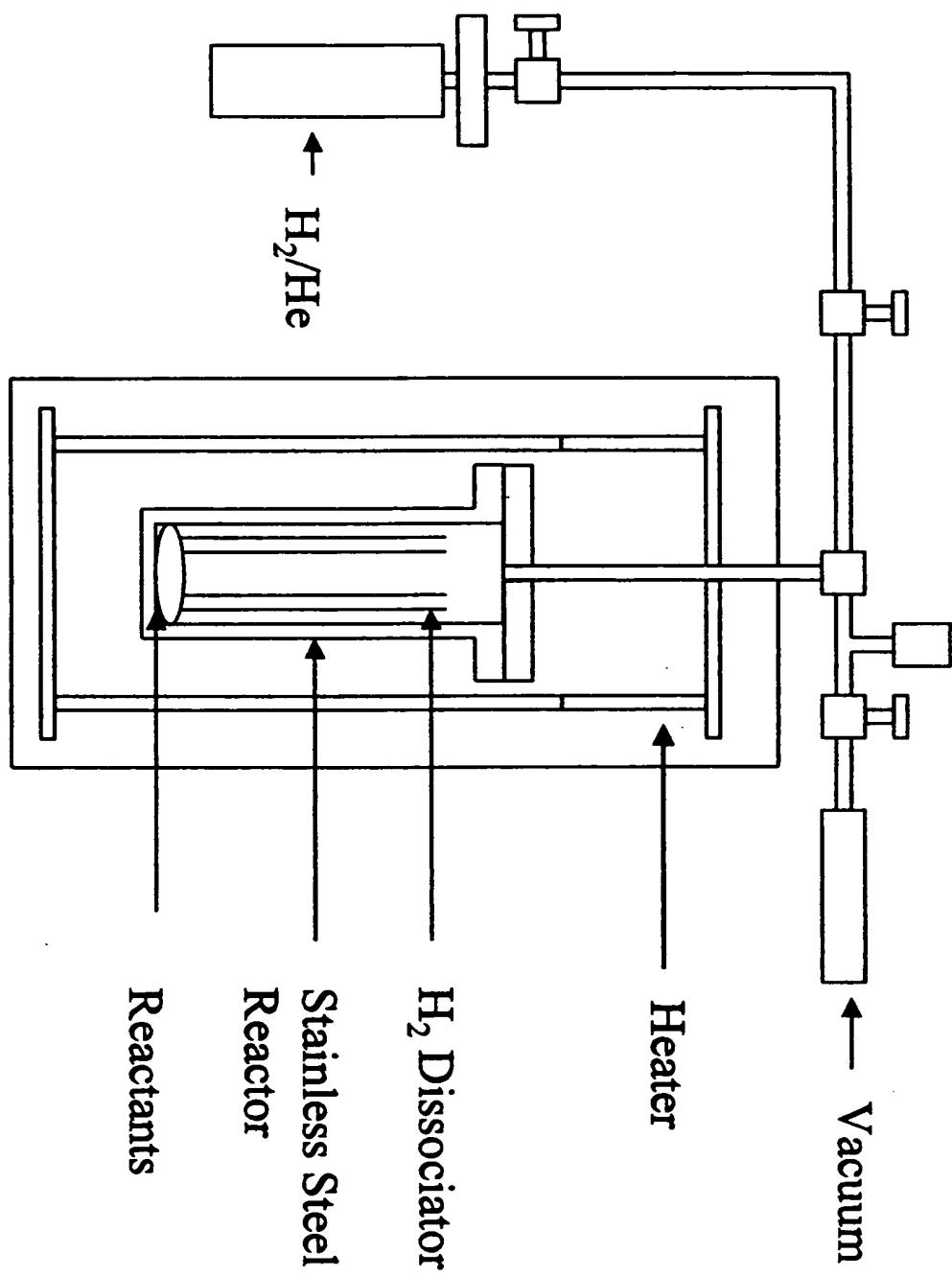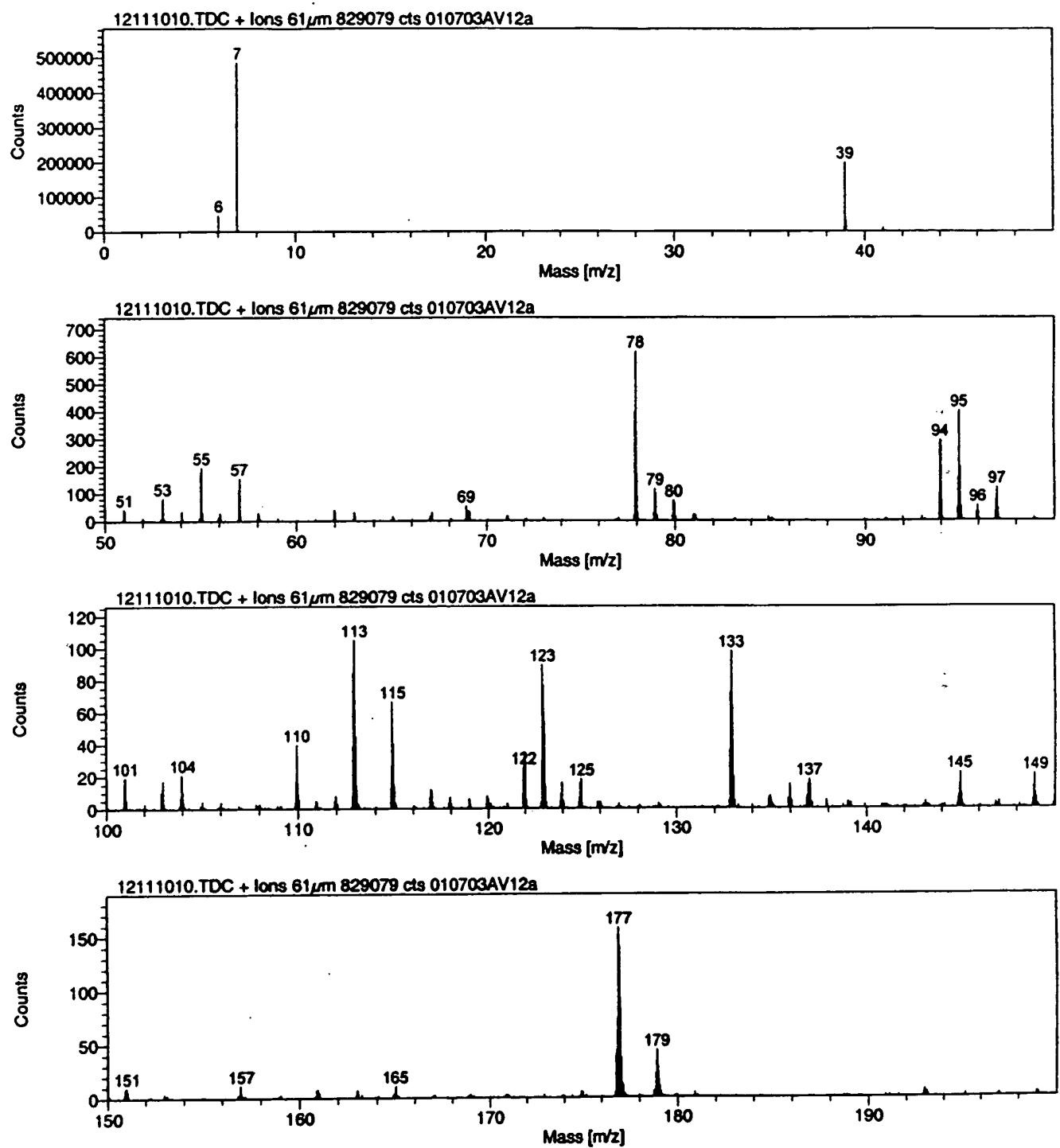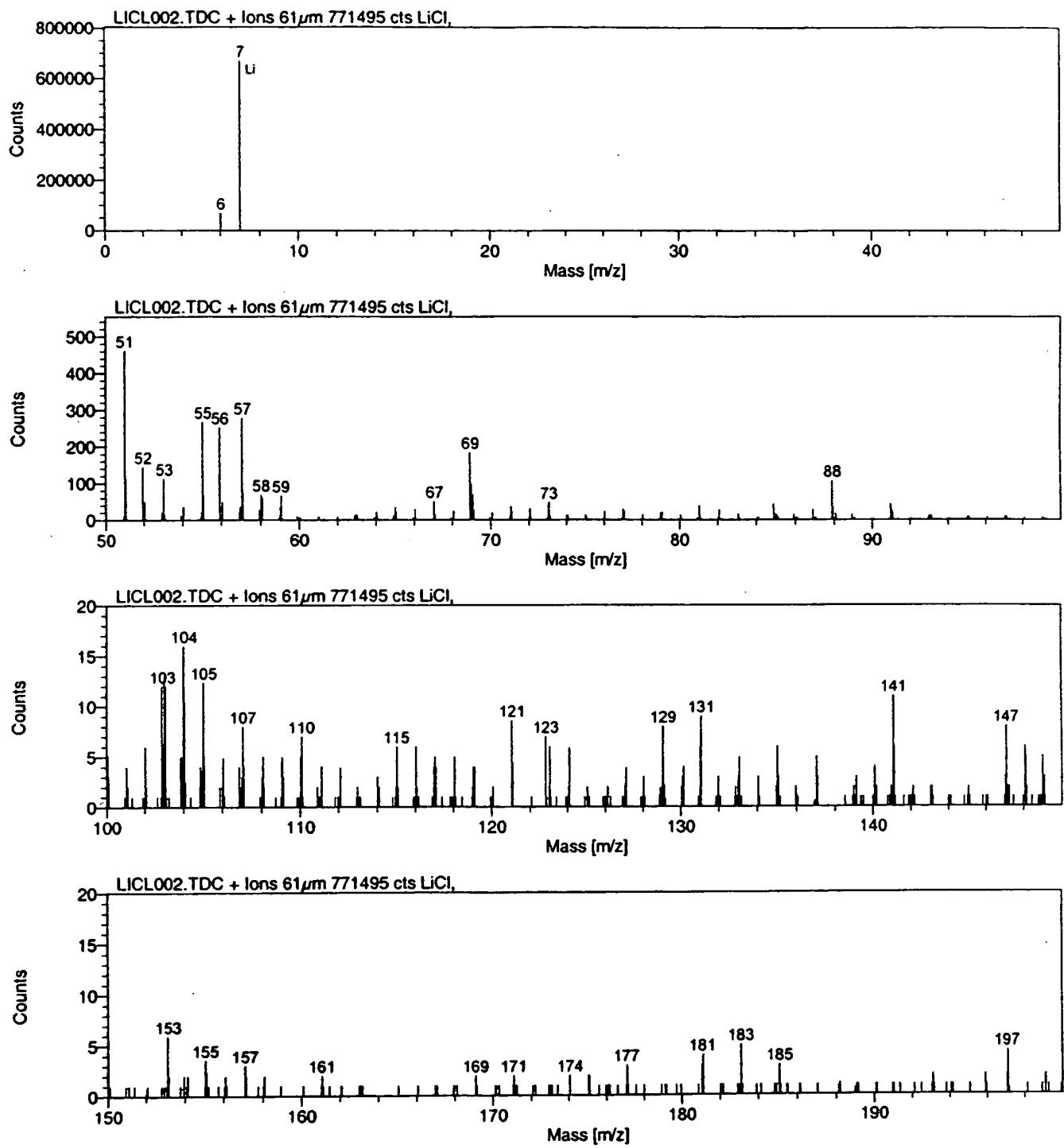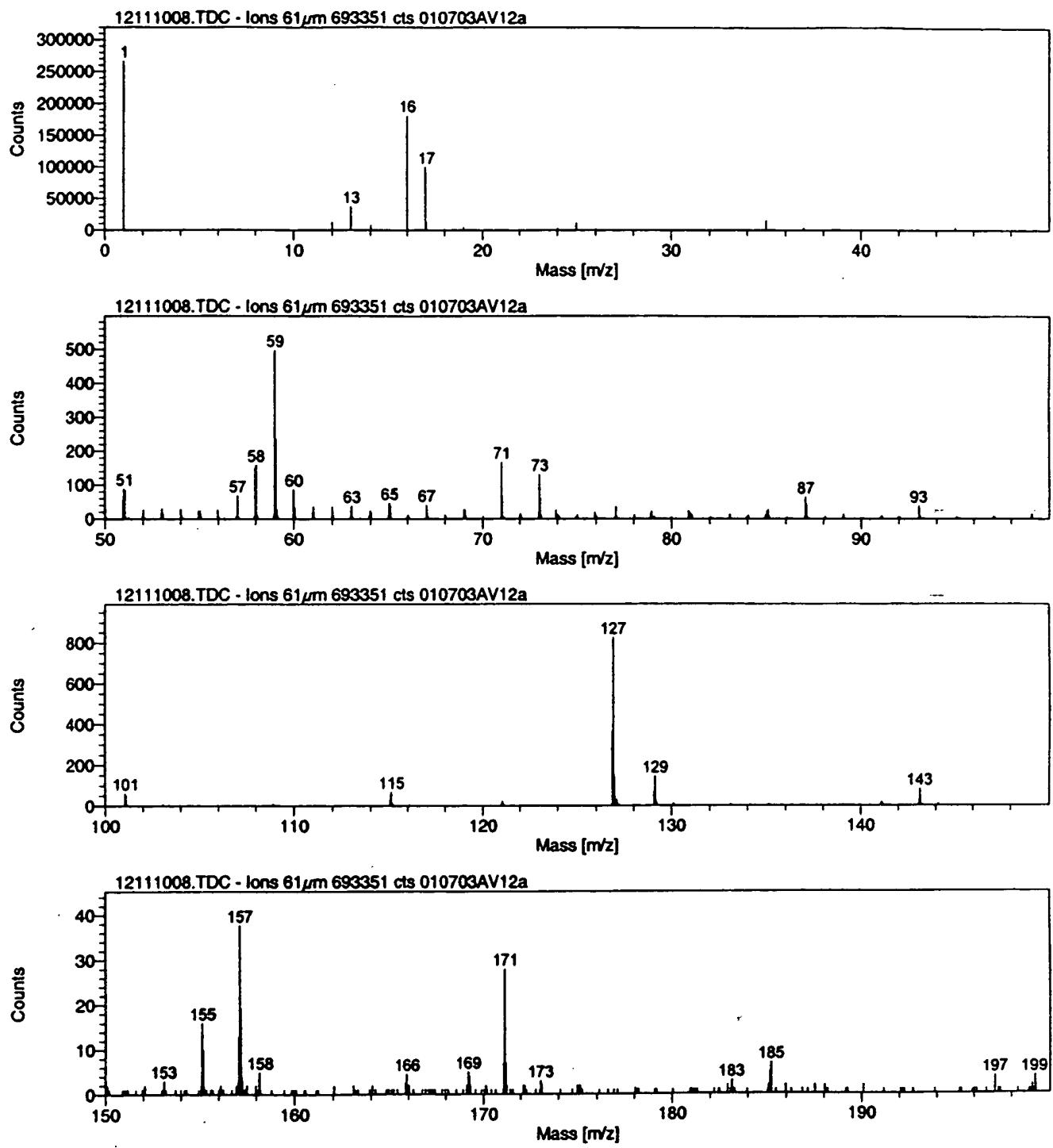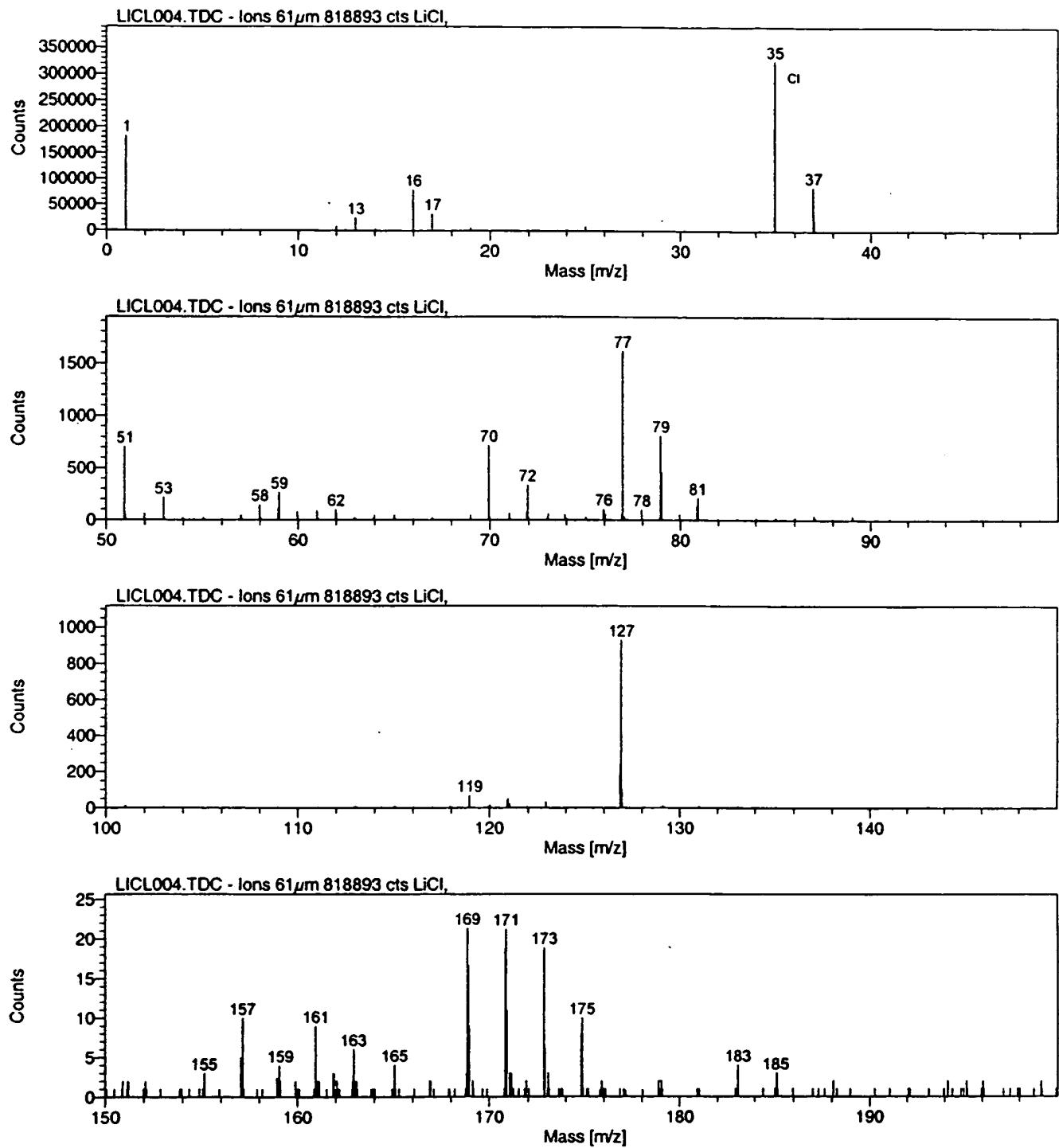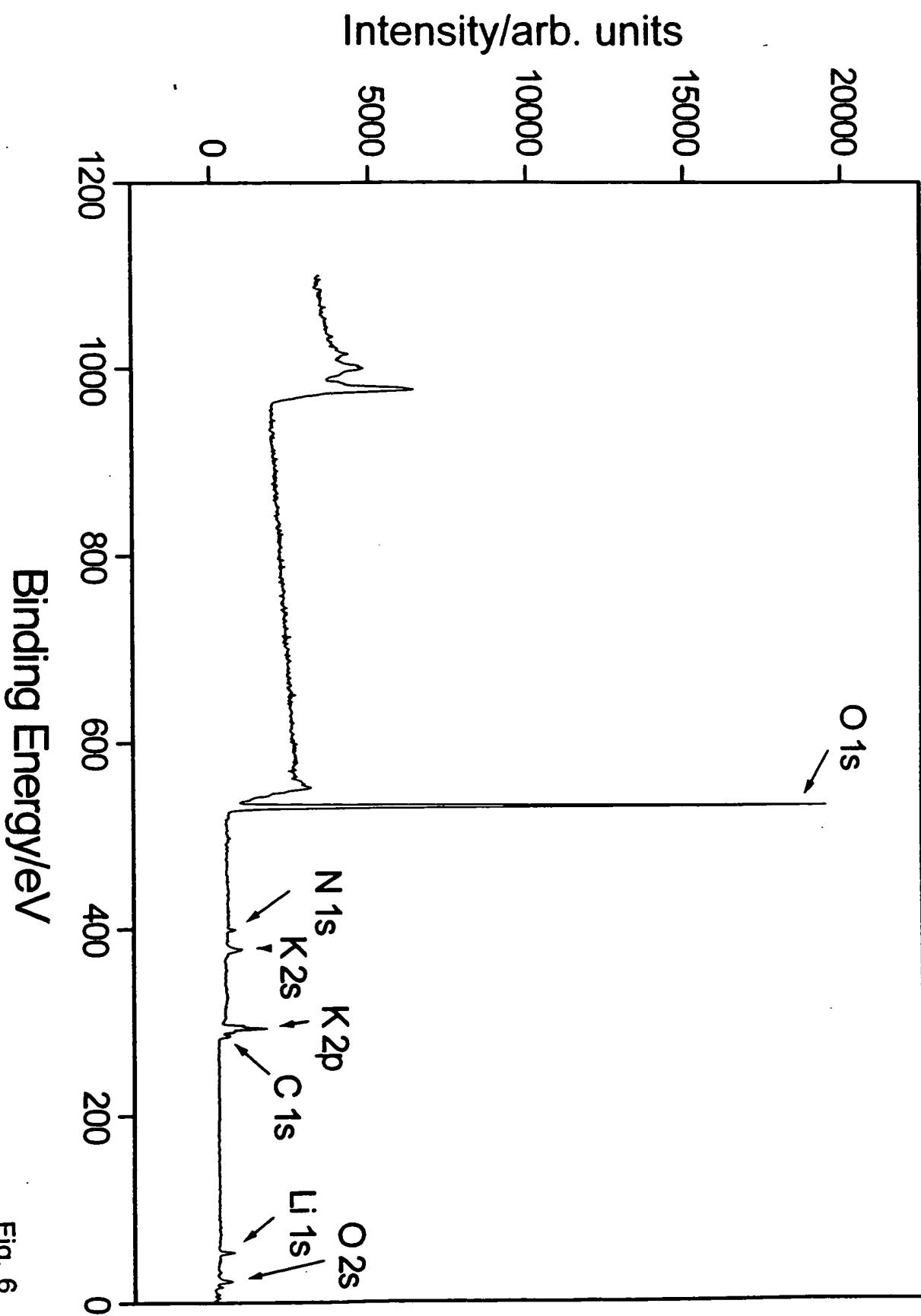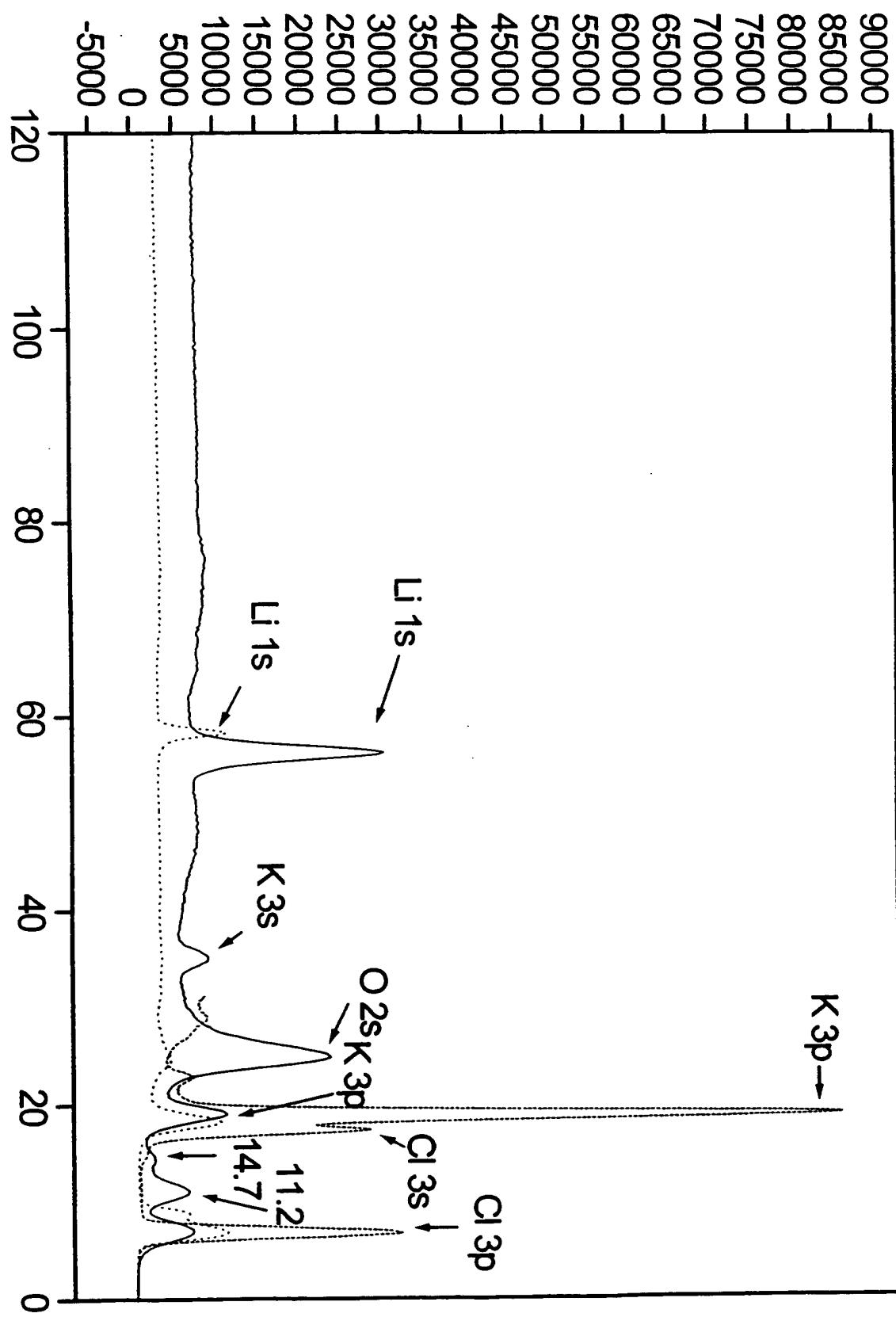
Binding Energy (eV)

Fig. 11

Fig. 12

Fig. 13

Fig. 14